Transverse motion of cohesive powders in flighted rotary kilns: experimental study of unloading at ambient and high temperatures

Marie Debacq, Stéphane Vitu, Denis Ablitzer, Jean-Léon Houzelot, Fabrice Patisson

TRANSVERSE MOTION OF COHESIVE POWDERS IN FLIGHTED ROTARY KILNS: EXPERIMENTAL STUDY OF UNLOADING AT AMBIENT AND HIGH TEMPERATURES

Marie DEBACQ[a,b,1], Stéphane VITU[c], Denis ABLITZER[a], Jean-Léon HOUZELOT[b], Fabrice PATISSON[a]

[a] Institut Jean Lamour (UMR 7198) - Département Science et Ingénierie des Matériaux et Métallurgie (SI2M), École des Mines de Nancy, Parc de Saurupt, CS 14234, 54042 Nancy cedex, France

[b] Laboratoire de Réactions et Génie des Procédés (UPR 3349), École nationale supérieure des industries chimiques (Ensic), 1 rue Grandville, BP 20451, 54001 Nancy cedex, France

[c] Laboratoire de Génie des Procédés pour l'Environnement, l'Énergie et la Santé (EA 21), Conservatoire National des Arts et Métiers (Cnam), case 2D1P20, 292 rue Saint-Martin, 75141 Paris cedex 03, France

DOI: 10.1016/j.powtec.2013.04.007 Powder Technology 245 (2013) 56-63

Corresponding author

Dr. Marie DEBACQ (marie.debacq@cnam.fr), Cnam-EA21, case courrier 2D1P20, 2 rue Conté, 75003 Paris, France. +33 1 58 80 87 07

Abstract

The transverse flow of cohesive powders in rotary kilns equipped with lifters was studied experimentally and theoretically. A laboratory device was built up in which the flow of uranyl difluoride (UO_2F_2), uranium sesquioxide (U_3O_8) and uranium dioxide (UO_2) powders was filmed, recorded, and analyzed using partly manual image analysis techniques. Experiments were performed both at room temperature and at high temperature. A constitutive law describing the powder discharge was derived, involving a relationship between the volume fraction of powder contained in a lifter and the angular position of this lifter. This law based on geometrical calculations is successfully compared to the experimental results of unloading.

Keywords

rotary kiln; cohesive powder; lifter; transverse motion; discharge; uranium

Highlights

►Transverse flow of cohesive powder in flighted rotary kiln is experimentally studied.
►Cohesive powders (uranyl difluoride and uranium oxides) are employed.
►Measurements are interpreted using partly manual image analysis techniques.
►The effect of kiln hold up, rotational speed and temperature are presented.
►A geometrically calculated flight unloading law is compared to experimental results.

Note

The results and calculations presented here were obtained in 1998 during a confidential study.

[1] Present address: Laboratoire de Génie des Procédés pour l'Environnement, l'Énergie et la Santé (LGP2ES - EA 21), Conservatoire National des Arts et Métiers (Cnam), case 2D1P20, 292 rue Saint-Martin, 75141 Paris cedex 03, France

1. INTRODUCTION AND BACKGROUND TO THE PROBLEM

For over a century [1], rotary kilns have been widely used in the inorganic chemistry industry. They are a key element in the production processes of cement, lime and pigments (titanium dioxide calcination) and in extractive metallurgy for the reduction of ore [2]. Rotary kilns are well suited for drying [3-4], for the pyrolysis of solid waste [5], and are also used to convert uranium fluoride into uranium dioxide for the manufacture of nuclear fuel [6-8].

Natural uranium cannot be processed directly because its content in isotope 235, the only fissionable isotope, is too low. To enrich the mineral, the uranium is therefore first converted into uranium hexafluoride (UF_6). Enrichment in isotope 235 is carried out in the gas phase, either by gaseous diffusion or by centrifugation. The depleted uranium is then converted into a chemically stable and insoluble oxide, U_3O_8, and stored. The enriched uranium is converted into solid UO_2 used to produce the solid fuel for nuclear power plants. Both processes are conducted in conversion kilns, which comprise a hydrolysis reactor and a rotary kiln fitted with lifters. Rotary conversion kilns are externally heated by resistors located close to the outside wall of the rotating cylinder, but they differ in size and nominal operating conditions [6]: the type of rotary kiln used for depleted uranium conversion is henceforth named "kiln #1"; the type of rotary kiln that converts enriched uranium is named "kiln #2".

Various studies have been carried out on conversion kilns in an attempt to simulate their hydrodynamic, chemical and thermal behavior [6]. In this type of kiln, hydrodynamic, thermal and chemical modelling processes are closely linked, as it is clear that heat and mass transfer processes are strongly governed by the transverse flow of the powder (i.e. in a cross section of the kiln), which determines the quality and duration of gas/solid contact. In order to correctly model the operation of the kiln, it is essential to be able to calculate precisely the solid distribution at any point in the rotary kiln. Understanding the solid motion taking place in rotary kilns is therefore crucial.

Numerous publications describe the flow of a solid charge in rotary kilns; the most frequently cited concerning transverse motion are Henein [9] and Mellmann [10]. Fewer studies have been devoted to the transverse movement of a solid charge in a rotary kiln equipped with lifters. A "lifter discharge law" (i.e. a relationship between the volume fraction of powder contained in a lifter and the angular position of this lifter) was first of all determined theoretically, and then verified experimentally. Based on this law, the gas/solid contact area and the mean residence time in the rotary kiln were calculated.

Thus Kelly [11] experimentally verified the law proposed by Schofield [12] giving the "instantaneous angle of repose of particles in a flight" as named by Kelly or "angle particles in flights make with horizontal" as called by Schofield (what we henceforth name "avalanche angle" δ) as a function of the dynamic friction coefficient: Kelly showed that for small enough rotational speeds, δ is constant for a given material whatever the angular position γ of the lifter. Based on the balance of forces, Blumberg [13] assumed that the surface of the powder in a lifter constantly forms the dynamic angle of repose θ_{dyn} with the horizontal (i.e. $\delta = \theta_{dyn}$); he experimentally verified that the volume of powder contained in a lifter varies linearly with its angular position γ (see notations on Fig. 1-a).

Several authors [14-18] used a description of the flight holdup with a constant avalanche angle as determined by Kelly in order to predict the overall particle movement in flighted rotary drums (mean residence time and RTD); the experimental work carried out in some of these studies generally concerns measurement of the mean residence time and/or the RTD. Baker [3] or Kelly [4] proposed methods to determine by calculation the best shape and the optimal number of lifters for drying applications.

Sherritt [19] proposed a method to calculate the hold up in a lifter. This method is not based on the avalanche angle but can only be applied to free-flowing granular materials.

A few authors [18, 20-22] calculated a non-linear discharge law based on Kelly's hypothesis of a constant avalanche angle. The small number of experimental results reported in the literature concern relatively coarse (usually on the order of a mm or more) and generally non cohesive particles, such as sugar, sand, granulated fertilizers, adsorbent beads or flexible filamentous particles [23]. Lee [24] presented an experimental study of the effect of certain operating parameters on this non-linear discharge law for a single lifter. Ajayi [25-26] recently published experimental studies using image analysis techniques to determine the loading conditions of sand in the lifters of a dryer; the study focused on quantifying the airborne solids. Sunkara [27] has very recently published a method for the calculation of the discharge characteristics of

rectangular flights identical to what we did in 1998 (see Appendix), again with experiments on non cohesive particles (sand and glass beads) of respectively 0.2 and 0.7 mm.
In the literature, "avalanche angle" δ and "dynamic angle of repose" θ_{dyn} are indeed often merged, but as will be shown in this work, these two angles are not equal for cohesive powders (weather they can be measured exactly).

With the development of image analysis techniques, it appeared important to measure the lifter discharge law experimentally rather than simply apply Kelly's hypothesis (i.e. a constant avalanche angle) to calculate this law (that is to say, measure the volume fraction of powder contained in a lifter and the angular position of this lifter, in order to establish a relationship between them). To the best of our knowledge, no paper has been published regarding the transverse flow of fine cohesive powders in rotary kilns equipped with lifters. Moreover, in the open literature, the experimental studies on lifter discharge have always been performed at ambient temperature, despite the fact that the behaviour of a cohesive powder under high temperature may be significantly different from that at room temperature. A key point in our paper is that the cohesive powders studied are those encountered in the manufacture of nuclear fuel. Furthermore, the influence of temperature on the behaviour of these powders is studied between ambient temperature and 790°C.
We have also attempted to predict the law theoretically, from geometrical considerations. Knowledge of the lifter discharge law is particularly useful for studies of rotary kilns, since it enables calculation of the fraction of powder that is lifted for given conditions, seeing that the mass transfer between solid and gaseous reagents is different from that in the bulk (which is continuously stirred through lifters). We also need to calculate the thermal transfer areas between solid and wall or solid and gas.

2. EXPERIMENTAL METHOD AND APPARATUS

2.1. Flow at ambient temperature

The transverse flow of various powders (UO_2F_2, U_3O_8 type #1 and type #2, and UO_2) was studied at ambient temperature using two experimental devices. The first one, denoted drum #1, represents a slice of kiln #1. The second, denoted drum #2, represents a slice of kiln #2. For both drums, the diameter and the internal equipment are the same as in the corresponding industrial kiln; the length is 0.3 m. The dimensions of kilns and lifters are given in Table 1. Each has a glass front to enable visual observation. They can be placed on a chassis equipped with a motor and speed variator and are installed in a closed ventilated cabin, as shown on Fig. 2. Filling and emptying operations are performed under hermetic glove-box conditions. Powder motion is filmed with a digital video camera through the glass window. The properties of the different powders are given in Table 2. It can be seen that the oxides are clearly cohesive (Carr's index is more than 0.4 and the Hausner ratio is more than 1.4); UO_2F_2 is on the borderline of highly cohesive powders.
The ranges of variation of the experimental parameters were chosen to cover the operating conditions of industrial kilns. The transverse flow of UO_2F_2 and U_3O_8 type #1 powders was studied thanks to drum #1. 10 experiments were performed, varying the hold up between 4 and 24 % and the rotational speed between 2 and 5 rpm. The transverse flow of UO_2F_2, U_3O_8 type #2 and UO_2 powders was studied thanks to drum #2. 12 experiments were performed, varying the hold up between 4 and 11 % and the rotational speed between 5 and 7 rpm. The lifting devices used can be seen on Fig. 1-b; drum #1 has six lifters, and drum #2 four.

The films recorded during the experiments were used to measure the volume fraction ξ occupied by the powder contained in a lifter (with respect to the total volume of the drum) as a function of its angular position γ, that is the "lifter discharge law". They also enabled the determination of three particular angular positions corresponding to the detachment angle γ_D, the start of effective discharge γ_I ("effective" with reference to mass transfer between solid and gaseous reagents) and the end of discharge γ_F (see notations on Fig. 1-a).
γ_D is the lifter position for which the powder it contains is no longer in contact with the powder remaining in the bottom of the drum. γ_I is the lifter position when the first powder particle leaving the lifter effectively encounters the gas; this is comparable to the First Unloading Flight (FUF) mentioned by Ajayi [25-26].

Finally, γ_F is the lifter position at which the last powder particle falls. In other words, for $\gamma < \gamma_D$, the lifter is inside the powder at the bottom of the drum; for $\gamma = \gamma_D$, the lifter moves out of the powder bed at the bottom of the drum; for $\gamma_D < \gamma < \gamma_I$, the particles leaving the lifter do not traverse the gas phase, but simply slide over the lifter and wall. For $\gamma = \gamma_I$, the first powder particle traverses the gas phase; for $\gamma_I < \gamma < \gamma_F$, the lifter gradually discharges its load through the gas; for $\gamma = \gamma_F$, the last powder particle leaves the lifter; and finally, at $\gamma > \gamma_F$, the lifter is empty.
Such observations are important for further studies: γ_D is appropriate when considering mass transfer between solid and gaseous reagents, while γ_I is suitable when calculating thermal transfer areas between solid and wall or solid and gas.

For each experiment, corresponding to about two minutes of film after reaching steady state, four image sequences were extracted. The first sequence contains one image per second and was used to measure the quantity of powder contained in each lifter and its corresponding position (for each experiment, about 50 to 100 measurements of ξ vs γ couples were made). The second sequence of images concerns the detachment of the lifters from the bed, while the third series represents the start of effective discharge. Finally, the fourth sequence shows the end of discharge. The second, third and fourth image sequences were used to measure the angles γ_D, γ_I and γ_F (for each experiment, at least 10 images catching each of these three particular situations were analysed).

Images from the first sequence were analysed semi-automatically using the Aphélion software, together with a specially developed measuring and processing algorithm. The lifter position was manually defined with respect to the horizontal. Both chassis and video camera were always placed perfectly horizontal (spirit levels), in order to ensure that a horizontal line of pixels on the image corresponded to the horizon. The quantity of powder contained in a lifter was determined by measuring the area of powder in contact with the glass face (due to the fact that the powder tended to stick to the window and to leave shadows on it, and considering the modest performances of image analysis' softwares at the time these measurements were made (1998), this area was manually delineated). During the experiments, it was visually checked that the quantity of powder contained in a lifter was the same at all cross sections of the drum and that contact with the glass did not affect the amount of powder lifted even though the particles were fine-grained. The volume fraction (with respect to the total volume of the drum) occupied by the powder $\xi(\gamma_k^i)$ contained in lifter number k located at position i (corresponding to an angle γ_k^i) was obtained by dividing the area manually delineated by powder in contact with the glass face by the cross sectional area of the drum. The analysis performed on this image sequence is given in detail in the chart shown in Fig. 3. Typical images of the loading of lifters are shown on Fig. 4 for both types of kiln: powders being cohesive, the lifters are widely overloaded at small angular positions, even at relatively small kiln hold up.
The second, third and fourth series of images were analysed using the software Vision Explorer MA. The angles at the end of discharge γ_F, the detachment angles γ_D and the angles at the start of effective discharge γ_I were measured with respect to the horizontal on at least ten different images for each of the 22 experiments.
With this method, the ξ vs γ curve is obtained, which is valid between γ_I and γ_F (or γ_D depending on the use of these results), and its intersection γ_F with the abscissa is perfectly defined. To calculate the quantity of powder present in the gas phase, γ_I will be used, whereas to calculate the total quantity of powder lifted at any time, γ_D will be employed. However, the disadvantage of γ_D is that it theoretically depends on the kiln hold up Z. Nevertheless, we will see in the following section (RESULTS) that, in our case, the bulk powder tends to split, forming a "bean" (see Fig. 5), so that in practice, γ_D is not highly dependent on Z.

2.2. Characteristic angles

The avalanche angle δ was measured for each type of powder in drums #1 and #2, at various hold up and rotational speeds. The previous films were re-used - the first image sequence was again analysed using the Vision Explorer MA software. The avalanche angle was measured for various lifter positions.

The static angles of repose for the four powders were measured using the crumbling cone method (NF T 20-221 standard), in which the powder is fed through a funnel, forming a cone whose angle is measured.
The dynamic angles of repose for the four powders were measured by the rotating cylinder technique, using drums #1 and #2 without their lifting devices. 16 experiments were performed, with hold up ranging between 7.5 and 16 % and rotational speed from 2 to 10 rpm. Each experiment was filmed for about two minutes after reaching steady state and one image every five seconds was extracted for analysis. The dynamic angles of repose were measured from the images using the Vision Explorer MA software.

2.3. Flow at the temperatures encountered in industrial processes

Since the behaviour of the solid charge under real process conditions may be different to that at room temperature, it is necessary to study the effect of temperature on lifter discharge. A complete high temperature system in which it is possible to film the powder behaviour is difficult to implement, particularly in the case of dangerous products such as uranium oxides. An appropriate static furnace was therefore equipped with a single rotating lifter system mounted on an axis (afterwards denoted single-lifter-device), in order to quantify the discharge behaviour: a rectangular flight forms two sides of a kind of "box", the extremities of the "box" correspond to the back of the drum and to its glass window, the last side of the "box" corresponds to the wall. Experiments were performed on the different types of powder, both at ambient temperature, to verify that the results were comparable to those obtained in the rotating drum, and at temperatures in the range encountered in industrial processes. This system is similar to the one recently used by Lee [24], except that in our case the lifter is placed in a furnace. The lifter is filled with pre-heated powder and then rotated, with periodic (every 5°) measurements of the weight of fallen powder and of the angle of inclination of the lifter, in order to derive the ξ vs γ curve.

3. RESULTS AND DISCUSSION

The lifters transport large quantities of powder and discharge very gradually, inducing highly efficient contact between the powder and the gas phase. Typical images are shown in Fig. 5.

3.1. Room temperature discharge law

For all the powders studied, the volume of powder contained in a lifter decreases linearly with the angle characterising its position (see Fig. 6). No significant influence was observed of the rotational speed, the type of powder, or even the drum concerned, on either the slope of the discharge law or on the initial and final discharge angles. Somewhat unexpectedly, the detachment angle was not affected by kiln hold up in the range $4 \leq Z \leq 25$ %, since for small hold up, the powder bed at the bottom of the drum does not take the form of a segment of a circle, but rather a "bean" shape, as illustrated in Fig. 5.
The discharge law, giving the volume fraction ξ occupied by the powder contained in a lifter (with respect to the total volume of the drum) as a function of the lifter's angular position γ, is given by the equation $\xi = 0.00012.(\gamma_F - \gamma)$. This law is valid between γ_D and γ_F in the case of the total quantity of powder raised at any time, or between γ_I and γ_F for the total quantity of powder falling through the gas at any time. The characteristic angles γ_D, γ_I and γ_F vary only slightly with the operating parameters in the ranges considered and no significant variation is observed between the different powders; their mean values and the standard deviations for all the experiments on the different powders, at different hold up and rotational speeds (a total of more than 200 images were considered to determine each angle) being:

- ✓ γ_D = -18° (-17.7° with a standard deviation of 7.4°) for the detachment angle;
- ✓ γ_I = -2° (-2.0° with a standard deviation of 6.3°) for the angle at the start of effective discharge;
- ✓ γ_F = 131° (131.2° with a standard deviation of 3.2°) for the angle at the end of discharge.

Regarding the slope of the discharge law, among the 22 experiments made, with about 50 to 100 measurements of ξ vs γ couples for each experiment, the mean value of the slope is $-0.000124^{\circ-1}$ with a standard deviation of $0.000025^{\circ-1}$.

However, for very small kiln hold up ($Z < 4\%$), the lifters cannot be totally filled, and at small angles, the volume of powder in the lifter is lower than when the kiln is sufficiently filled (empty diamonds on Fig. 6).

For high hold up, the lifter fills more at small angles than for medium kiln hold up (black triangles on Fig. 6). For very low or very high kiln hold up, the shape of the discharge curve is therefore modified at small angles (up to about 5°), as well as γ_D and γ_I. The γ_F angle (end of discharge) remains unchanged.
Finally, it should be noted that, for discharge during a single revolution, the flow of U_3O_8 and UO_2 powders at ambient temperature is jerky (empty squares on Fig. 6), in agreement with the qualitative observation that these powders tend to fall irregularly, in clumps.

3.2. Characteristic angles

3.2.1. Avalanche angles

In the case of the cohesive powders studied, the surface of the powder bed inside a lifter is not planar, as can be seen in Fig. 5. The avalanche angle δ, defined as that between the median plane of this non-planar surface and the horizontal, These measurements show wide scatter, and are rarely close to the dynamic angle of repose (see values in Table 2). The mean value of the avalanche angle is 68°, and is not affected by the type of powder considered. 92% of the measured values for δ lie between 40 and 90°, but only 30 % are between 63 and 73°.

3.2.2. Static and dynamic angles of repose

The static angle of repose values for the four powders are given in Table 2.
The bed surface was not always perfectly planar during measurement of the dynamic angles of repose (see Fig. 5): thus the dynamic angles of repose were measured from ±3° to ±13° over all 16 experiments by varying hold up and rotational speed. On some pictures, the bed surface is roughly planar: in these cases defining θ_{dyn} is not a problem; in other cases (when the bed surface forms a "bean"; rarely on oxides, most commonly on UO_2F_2), two angles can be defined as shown on Fig. 5c, which led to the variability of the measurements mentioned in Table 2.
For the uranium oxide powders, the static angle of repose θ_{stat} is about 10° larger than the dynamic one θ_{dyn}. In contrast, for UO_2F_2, θ_{stat} is roughly equal to θ_{dyn}.

3.2.3. Modelling of lifter discharge

Based on the expressions given in Appendix, the variation in the fraction of powder present in a lifter was calculated as a function of its angular position and the predicted results were compared to the experimentally determined values.
Considering the wide scatter in the measured avalanche angle mentioned in section 3.2.1, several values of δ were tested, namely the mean measured value (68°) and the value calculated from γ_F (= 131° as reported in the previous section of this paper), i.e. $\delta = \gamma_F - 90° = 41°$. We can see that the theoretical curves obtained when using the mean measured value of δ and $\delta = \gamma_F - 90$ enclose the majority of data points; we therefore also plotted the theoretical curve corresponding to the mean of the two previous values, i.e. $\delta = 55°$ (thick line). As can be observed in Fig. 9, experimental results are satisfactorily represented by the theoretical approach. It may be noted that the value of the dynamic angle of repose does not either allow to correctly represent the experimental points. ($\delta \neq \theta_{dyn}$).
Finally, it should be emphasized that the laws indicated in Table A1 can be readily extended to other lifters of similar shape. Indeed, the principle of the calculation is general and could be applied to different lifter designs. Our model leads to a discharge curve that is very comparable to those obtained by Baker [3], Fernandes [21], Kelly [11], Revol [20], Van Puyvelde [22] and Sunkara [27]. In our case, the powders being cohesive, the definition of the portions of curves is different (more defined regions) as can be seen in Appendix on Fig. A1 and in Table A1.

3.3. High temperature discharge laws

During the high temperature tests with our experimental apparatus, it was not possible to fully load the lifter, due to the absence of a complete kiln wall. In industrial kilns (and therefore at high temperature), lifters are fully loaded. Consequently, the measurements at high temperature presented in Fig. 7 and 8 are representative only between $\gamma \approx 75°$ and γ_F.

As shown on Fig. 7, temperature has no significant effect on the discharge behaviour of UO_2F_2 (in the temperature range where UO_2F_2 does not decompose). The discharge law for UO_2F_2 up to 500°C can thus be given by the equation obtained at room temperature: $\xi = 0.00012.(\gamma_F - \gamma)$, between γ_I and γ_F.

In the case of both types of U_3O_8 and of UO_2, discharge begins much later at high temperature than at ambient temperature, but ends at the same γ_F as at room temperature, as can be seen on Fig. 8. During discharge, the powder behaviour is similar to that of a sandcastle being unmoulded. However, it can reasonably be assumed that at high temperatures the lifter is loaded in the same way as at room temperature for $\gamma = \gamma_D$; this gives the horizontal dotted line on Fig. 8. Through the few points available, we can plot a line from point ($\gamma = \gamma_F$; $\xi = 0$) giving an unloading slope at high temperature of $0.00035^{\circ -1}$ that is extrapolated up to the load obtained at room temperature when the filter leaves the bed ($\gamma = \gamma_D$). The intersection of this line gives a new angle of about 80° for the start of effective discharge γ_I' (see construction on Fig. 8). Thus, the discharge behaviour for both types of U_3O_8 and for UO_2 at 700-800°C is given by: $\xi = 0.00035.(\gamma_F - \gamma)$, between γ'_I and γ_F.

5. CONCLUSIONS AND PERSPECTIVES

A law describing the discharge of lifting devices used in industrial rotary kilns for defluorinating and reducing uranyl difluoride has been established both theoretically and experimentally. For the types of powders studied (UO_2F_2,U_3O_8 type #1 and type #2, and UO_2) and in the range of variation considered, no significant influence of the rotational speed, the kiln hold up (on condition that it is neither too high nor too low), the nature of the powder, or the kiln dimensions is observed. The temperature, however, does affect the discharge law of the oxides, which become highly cohesive at high temperatures.
In spite of the cohesive nature of the powders studied, and although the powder surface angle in the lifters is highly variable, the experimentally determined discharge law is approximately linear, as reported by Blumberg [13]. Moreover, it is possible to determine an "equivalent avalanche angle" capable of correctly representing the experimental measurements. The value of this angle (which is significantly higher than the dynamic angle of repose) will be extremely useful to calculate the various heat exchange areas in rotary kiln equipped with lifters.

The discharge law obtained can be used to calculate the average powder distribution in the lifters, in the gas phase and at the bottom of the kiln, for given operating conditions [28]. This information is necessary to determine the gas/solid contact time, the heat exchange areas and the mean residence time in the kiln. It is therefore an essential element for the establishment of a physical-chemical model of rotary kilns [29].

Acknowledgements
This work was supported by a grant from FBFC[2] Romans (France) and Cogema[3] Pierrelatte (France). We gratefully acknowledge André FEUGIER and Didier HARTMANN for their kind help in this work, and Alain HAZOTTE for his assistance in developing the image analysis program.

[2] Franco-Belge de Fabrication de Combustible
[3] Compagnie Générale des Matières Nucléaires

SYMBOLS USED

β [°]	angle characterising the contact between the powder and the kiln wall
δ [°]	avalanche angle (instantaneous angle of repose made by particles in a flight with respect to horizontal)
γ [°]	angular position of the lifter (with respect to the horizontal)
γ_A [°]	first limiting angular position
γ_B [°]	second limiting angular position
γ_D [°]	detachment angle
γ_F [°]	angle at the end of discharge
γ_I [°]	angle at the start of effective discharge (at room temperature)
γ_I' [°]	angle at the start of effective discharge (at the temperatures encountered in industrial processes)
h_o [m]	lifter dimension normal to the kiln wall
h_p [m]	lifter dimension parallel to the kiln wall
η_R [m^3 m^{-1}]	volume of powder contained in a lifter per meter of kiln length
θ_{dyn} [°]	dynamic angle of repose (measured in a rotating bare drum)
θ_{stat} [°]	static angle of repose (measured by the normalised crumbling cone method)
R [m]	kiln radius
ω [rpm]	rotational speed
ξ [-]	volume fraction occupied by the powder contained in a lifter (with respect to the total volume of the drum)
Z [-]	kiln hold up

REFERENCES

[1] R. K. Meade, The Development of the Rotary Kiln and Its Application to Various Chemical and Metallurgical Processes, Ind. Eng. Chem. 6(9) (1914) 754-760.

[2] A. A. Boateng, Rotary Kilns, Butterworth-Heinemann, Oxford, 2008.

[3] C.G.J. Baker, The design of flights in cascading rotary dryers, Drying Technol. 6(4) (1988) 631-653. doi: 10.1080/07373938808916402

[4] J. Kelly, Flight design in rotary dryers, Drying Technol. 10(4) (1992) 979-993. doi:10.1080/07373939208916491

[5] N. Descoins, J.L. Dirion, T. Howes, Solid transport in a pyrolysis pilot-scale rotary kiln: preliminary results—stationary and dynamic results, Chem. Eng. Process. 44(2) (2005) 315-321. doi:10.1016/j.cep.2004.02.025

[6] M. Debacq, Étude et modélisation des fours tournants de défluoration et réduction du difluorure d'uranyle, Ph.D. Thesis, Institut National Polytechnique de Lorraine, Nancy, France (2001).

[7] C. Nicole, Étude et modélisation de l'hydrofluoration du dioxide d'uranium en four tournant, Ph.D. Thesis, Institut National Polytechnique de Lorraine, Nancy, France (1996).

[8] P. Thammavong, M. Debacq, S. Vitu, M. Dupoizat, Experimental apparatus for studying heat transfer in externally heated rotary kilns, Chem. Eng. Technol., 34(5) (2011) 707-717. doi:10.1002/ceat.201000391

[9] H. Henein, J.K. Brimacombe, A.P. Watkinson, Experimental studies of transverse bed motion in rotary kilns, Metall. Trans. B 14B(2) (1983) 191-205. doi:10.1007/BF02661016

[10] J. Mellmann, The transverse motion of solids in rotating cylinders-forms of motion and transition behaviour, Powder Technol. 118(3) (2001) 251-270. doi:10.1016/S0032-5910(00)00402-2

[11] J.J. Kelly, J.P. O'Donnell, Dynamics of granular material in rotary dryers and coolers, Inst. Chem. Eng. 29 (1968) 34-44.

[12] F.R. Schofield, P.G. Glikin, Rotary Driers and Coolers for Granular Fertilizers, Trans. Inst. Chem. Eng. 40 (1962) 183-190.

[13] W. Blumberg, E.-U. Schlünder, Transverse bed motion and convective mass transfer in rotary cylinders. Part 2. With lifters, Chem. Eng. Process. 35(6) (1996) 405-411. doi:10.1016/S0255-2701(96)04151-7

[14] F.Y. Wang, I.T. Cameron, J.D. Litster, V. Rudolph, A fundamental study of particle transport through rotary dryers for flight design and system optimisation, Drying Technol. 13(5–7) (1995) 1261-1278. doi:10.1080/07373939508917021

[15] M.E. Sheehan, P.F. Britton, P.A. Schneider, A model for solids transport in flighted rotary dryers based on physical considerations, Chem. Eng. Sci. 60(15) (2005) 4171-4182. doi:10.1016/j.ces.2005.02.055

[16] P.F. Britton, M.E. Sheehan, P.A. Schneider, A physical description of solids transport in flighted rotary dryers, Powder Technol. 165(3) (2006) 153-160. doi:10.1016/j.powtec.2006.04.006

[17] J.P. Pan, T.J. Wang, J.J. Yao, Y. Jin, Granule transport and mean residence time in horizontal drum with inclined flights, Powder Technol. 162(1) (2006) 50-58. doi:10.1016/j.powtec.2005.12.004

[18] M.H. Lisboa, D.S. Vitorino, W.B. Delaiba, J.R.D. Finzer, M.A.S. Barrozo, A study of particle motion in rotary dryer, Braz. J. Chem. Eng. 24 (2007) 365-374. doi: 10.1590/S0104-66322007000300006

[19] R.G. Sherritt, R. Caple, L.A. Behie, A.K. Mehrotra, The Movement of Solids Through Flighted Rotating Drums. Part I: Model Formulation, Can. J. Chem. Eng. 71(3) (1993) 337-346. doi:10.1002/cjce.5450710302

[20] D. Revol, C.L. Briens, J.M. Chabagno, The design of flights in rotary dryers, Powder Technol. 121(2-3) (2001) 230-238. doi:10.1016/S0032-5910(01)00362-X

[21] N. J. Fernandes, C. H. Ataíde, M. A. S. Barrozo, Modeling and experimental study of hydrodynamic and drying characteristics of an industrial rotary dryer, Braz. J. Chem. Eng. 26(2) (2009) 331-341. doi:10.1590/S0104-66322009000200010

[22] D.R. Van Puyvelde, Modelling the hold up of lifters in rotary dryers, Chem. Eng. Res. Des. 87 (2009) 226-232. doi:10.1016/j.cherd.2008.08.018

[23] F. Geng, Y. Li, X. Wang, Z. Yuan, Y. Yan, D. Luo, Simulation of dynamic processes on flexible filamentous particles in the transverse section of a rotary dryer and its comparison with ideo-imaging experiments, Powder Technol. 207(1-3) (2011) 175-182. doi:10.1016/j.powtec.2010.10.027

[24] A. Lee, M.E. Sheehan, Development of a geometric flight unloading model for flighted rotary dryers, Powder Technol. 198(3) (2010) 395-403. doi:10.1016/j.powtec.2009.12.004
[25] O.O. Ajayi, M.E. Sheehan, Application of image analysis to determine design loading in flighted rotary dryers, Powder Technol. (2011). doi:10.1016/j.powtec.2011.05.013 – *article in press*
[26] O.O. Ajayi, M.E. Sheehan, Design loading of free flowing and cohesive solids in flighted rotary dryers, Chem. Eng. Sci. 73 (2012) 400-411. doi: 10.1016/j.ces.2012.01.033
[27] K.R. Sunkara, F. Herz, E. Specht, J. Mellmann, R. Erpelding, Modeling the discharge characteristics of rectangular flights in a flighted rotary drum, Powder Technol. 234 (2013) 107-116. doi:10.1016/j.powtec.2012.09.007
[28] M. Debacq, P. Thammavong, S. Vitu, D. Ablitzer, J.-L. Houzelot, F. Patisson, A hydrodynamic model for flighted rotary kilns used for the conversion of cohesive uranium powders. *submitted to Chem. Eng. Res. Des. on 06/10/2012*
[29] M. Debacq, S. Vitu, D. Ablitzer, J.-L. Houzelot, F. Patisson, A global model for flighted rotary kilns used for the convertion of uranium. *to be submitted to Chem. Eng. Sci. during summer 2013*

APPENDIX

In order to model the discharge law, we assume that all the lifters are fully filled and that the particle bed inside the lifters has a constant bulk density. If the avalanche angle δ is assumed to be constant, which is true for non-cohesive powders, it is possible, based on geometrical considerations, to calculate the quantity η_R of powder contained in a lifter per meter of kiln length as a function of its angular position γ. Let R be the cylinder radius, h_o and h_p the lifter dimensions (h_o is the dimension of the branch perpendicular to the wall and h_p the dimension of the branch parallel to the wall). The calculations generally involve an angle β (see definition on Fig. 1-b) representing the contact between the powder and the cylinder wall. The volume fraction ξ occupied by the powder contained in a lifter (with respect to the total volume of the drum) is obtained from η_R according to $\xi = \eta_R/(\pi.R^2)$.

Four domains, each with a different geometry, can be distinguished on Fig. A1; they are bounded by five particular positions. Let O be the centre of the drum, A the top edge of the powder and B and C the extremities of the lifter (see Fig. 1-b). For $\gamma_I \leq \gamma < \gamma_A$, the segment [AB] is located inside the triangle OAC. For $\gamma_A < \gamma < \delta$, the segment [AB] is situated outside the triangle OAC. For $\delta < \gamma < \gamma_B$, the segment [AB] is located inside the rectangle whose two sides are formed by the lifter. Finally, for $\gamma_B < \gamma \leq \gamma_F$, the segment [AB] is inside the right-angled triangle, two of whose sides are formed by the lifter.
For each of the domains defined above, and for each boundary position, the expression for the angle β was determined geometrically [6]. The surface delineated by the lifter and the wall together with that determined by the free surface of the powder were then calculated. The latter surface forms the angle δ with respect to the horizontal. The different expressions used to calculate the quantity of powder inside the lifter at a particular position are given in Table A1. Details of the calculations are given in the additional supporting information.

FIGURES

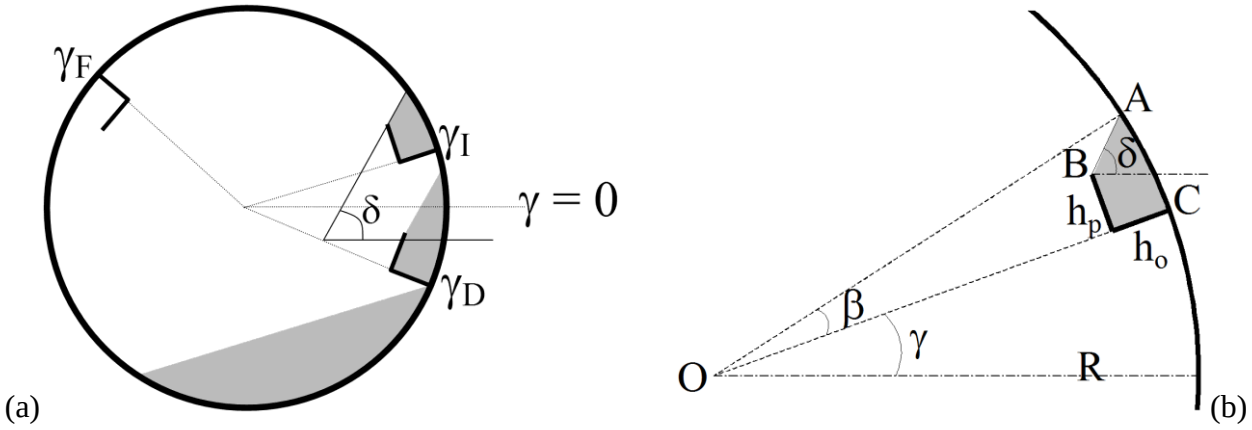

Fig. 1. Characteristic parameters for the discharge law (a); lifter parameters (b).

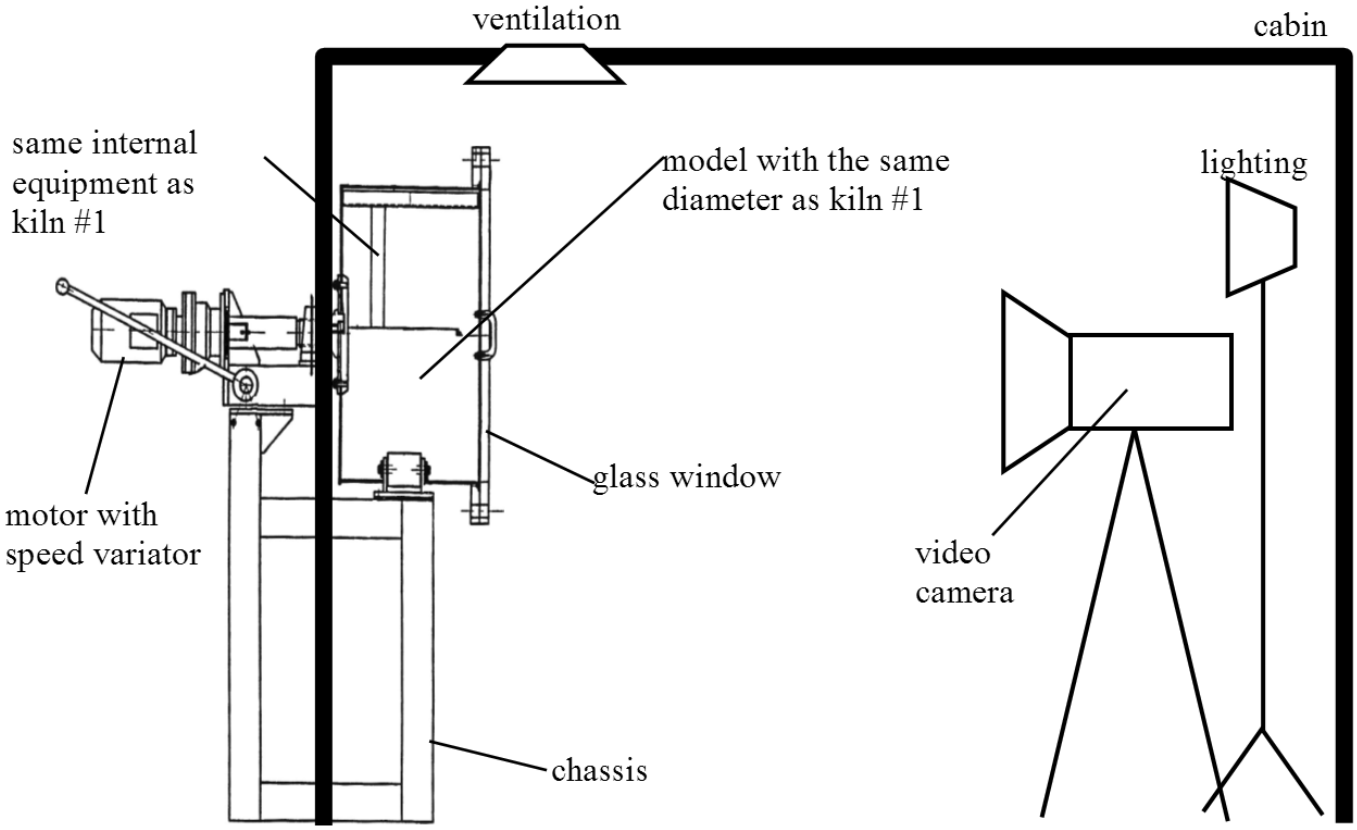

Fig. 2. Schematic representation of the apparatus (for example, with drum #1).

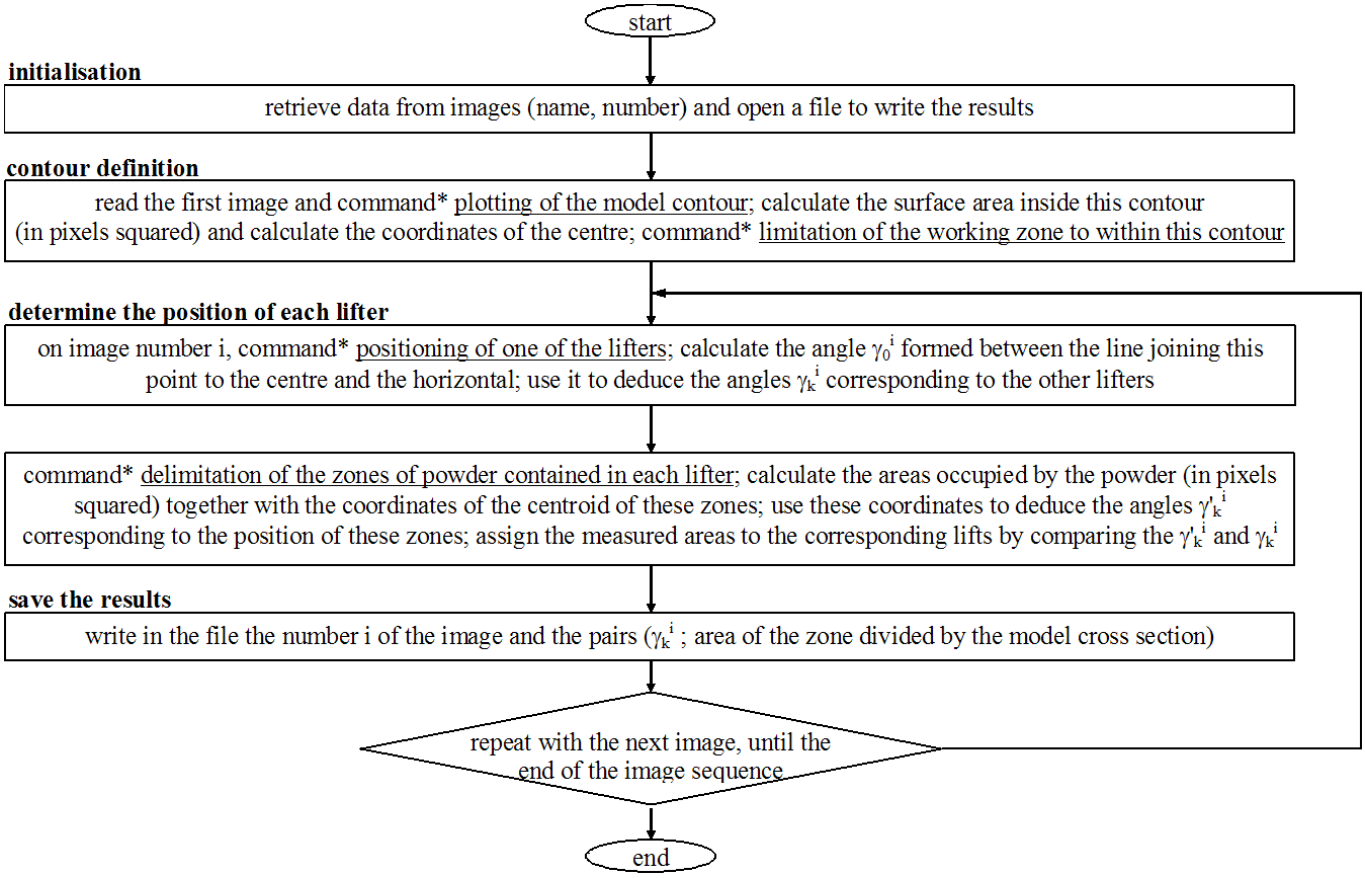

Fig. 3. Flow chart for the measurement processing algorithm (Aphélion software).
** "Command..." indicates operator intervention in the partly manual procedure.*

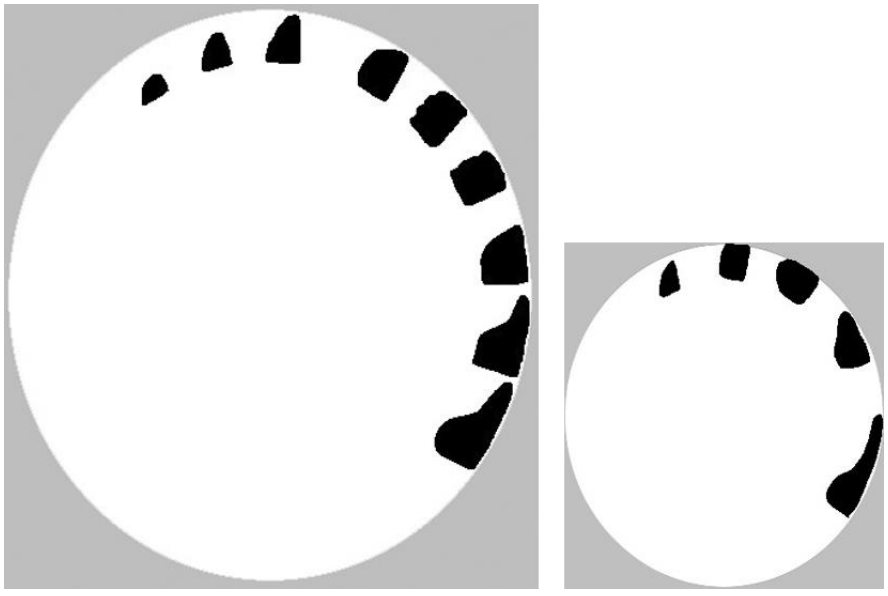

Fig. 4. Diagrams of successive positions of a lifter with its loading.
(left: U_3O_8 type #1 in drum #1; right: UO_2F_2 in drum #2)

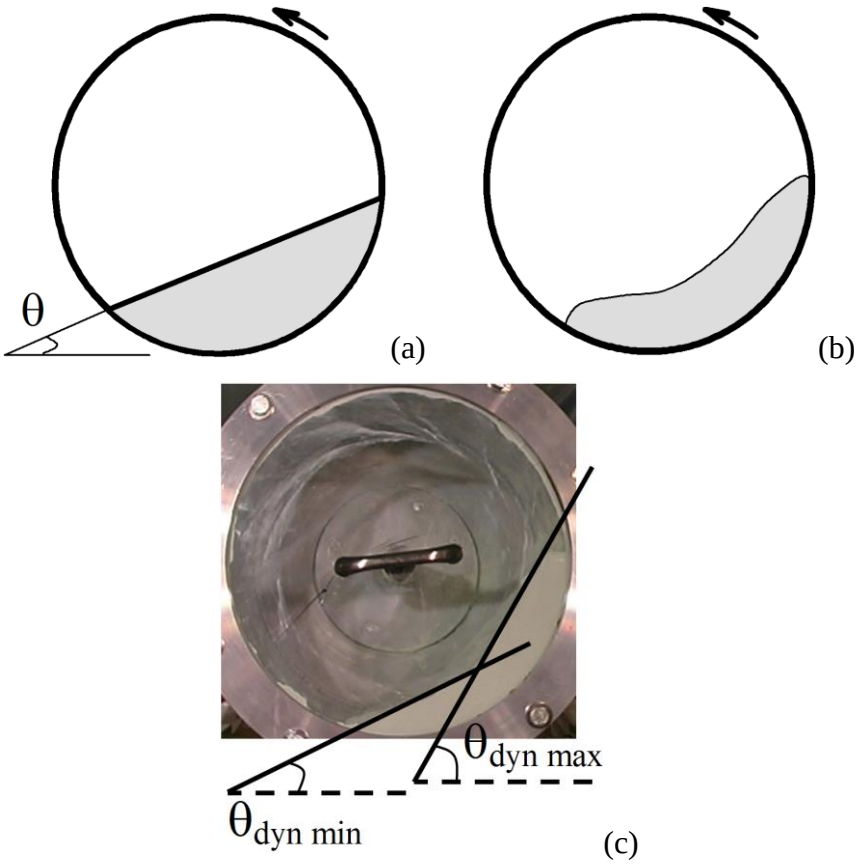

Fig. 5. Segment of a disc (a) and "bean" profile (b-c).
(photograph: UO_2F_2 in drum #2 without lifters; Z = 15%; ω = 3 rpm)

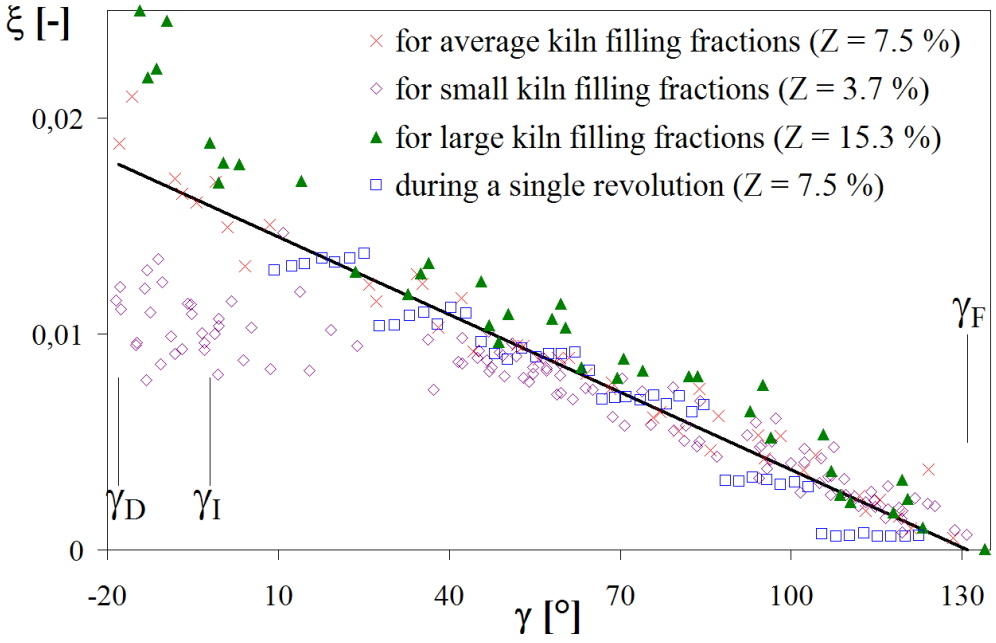

Fig. 6. Lifters' unloading at room temperature.
(U_3O_8 type #1 in drum #1; ω = 3 rpm)
The straight line corresponds to the average of all the tests conducted.

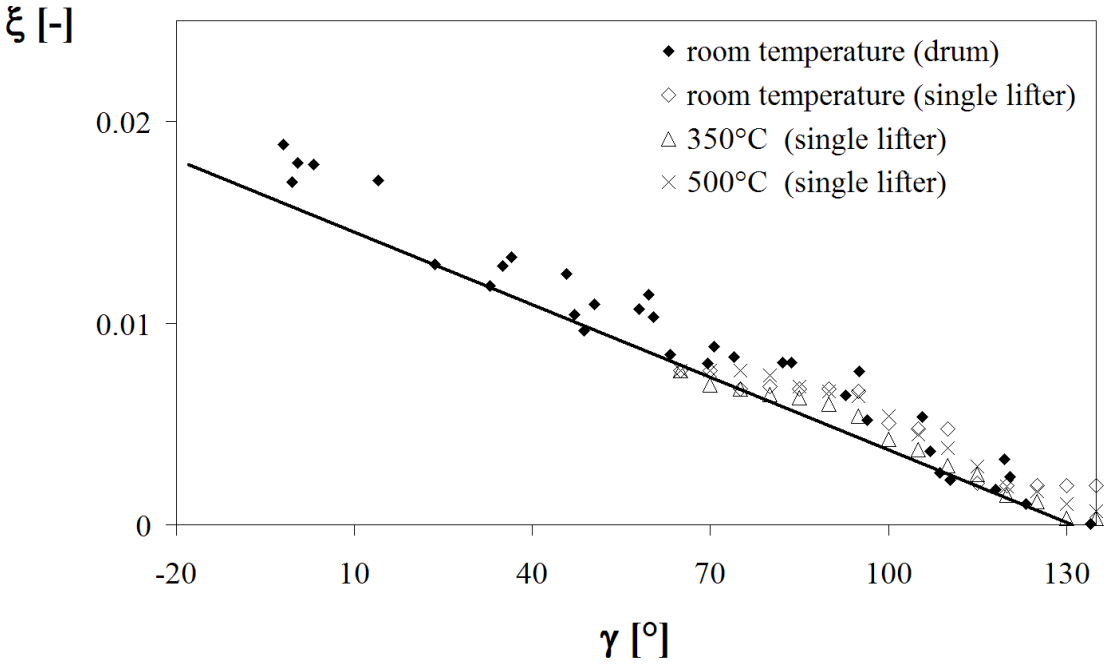

Fig. 7. Discharge of UO_2F_2.
(example for UO_2F_2 in the single-lifter-device; ω = 2 rpm)

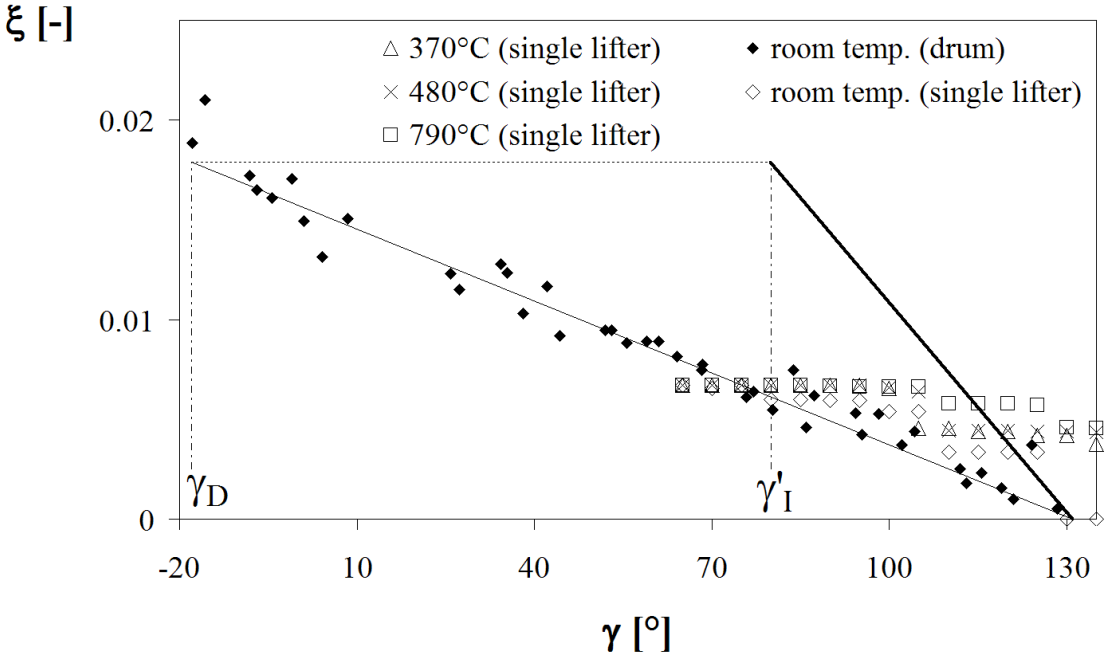

Fig. 8. Discharge of uranium oxide.
(example for U_3O_8 type #1 in the single-lifter-device; ω = 2 rpm)

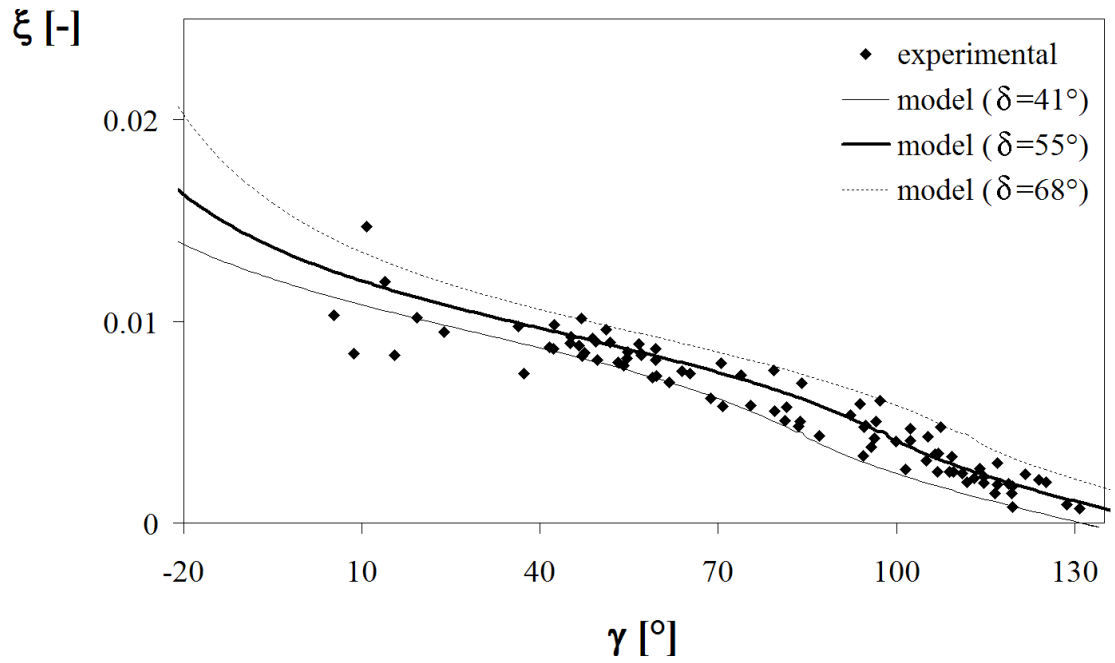

Fig. 9. Discharge law: comparison model / experiment.
(U_3O_8 type #1 in drum #1; Z = 3.7 and 7.5%; ω = 3 rpm)

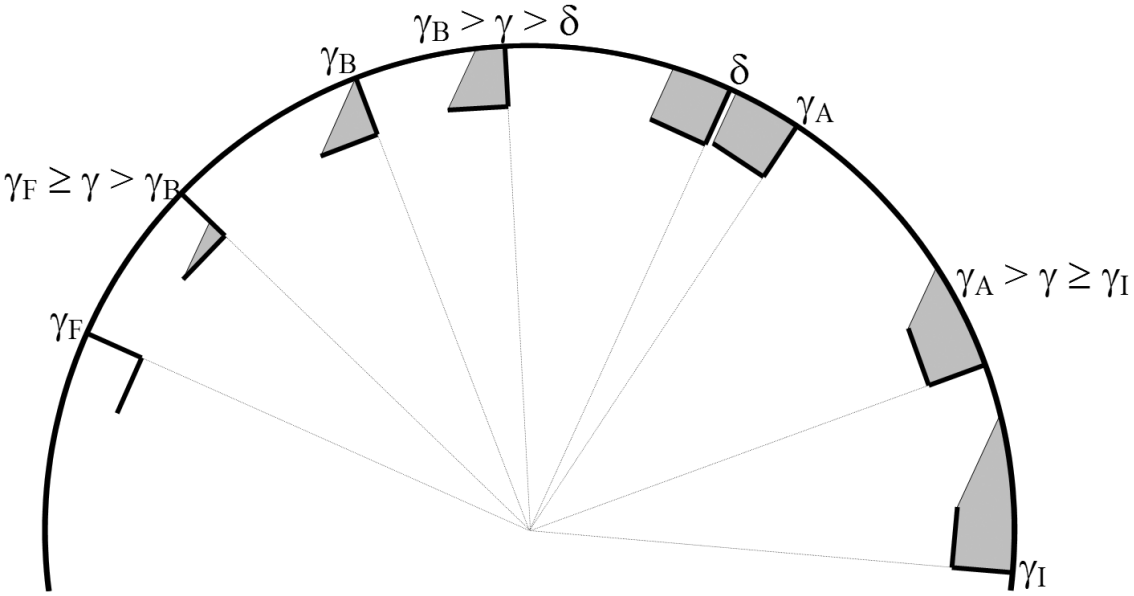

Fig. A1. The four domains for calculating ξ and limits of these domains.

TABLES

Table 1. Dimensions of the kilns.
* see Fig. 1-b.

	inside diameter [mm]	**length [m]**	**number of lifters**	**h_o* [mm]**	**h_p* [mm]**
kiln #1	750	10.24	6	60	60
kiln #2	348	5.34	4	35	35

Table 2. Properties of the different powders.

	UO_2F_2	**U_3O_8 type #1**	**U_3O_8 type #2**	**UO_2**
bulk density [kg m^{-3}]	380	1140	590	800
consolidated bulk density [kg m^{-3}]	470	2000	960	1630
grain size distribution [µm]	20 & 300	10 & 40	3 & 60	3 & 60
static angle of repose [°] θ_{stat}	43	50	51	45
dynamic angle of repose [°] θ_{dyn}	42 ± 11	33 ± 8	39 ± 3	33 ± 13°
Carr's index [-]	0.2	0.4	0.4	0.5
Hausner ratio [-]	1.2	1.8	1.6	2.0

The densities are measured by the method of the test tube (250 mL; inside diameter 39 mm). They are obtained ± 20 kg m^{-3}.
The particle size distributions of samples of oxides (U_3O_8 and UO_2) were measured with a COULTER 1.31 1.8 in water. UO_2F_2 particle size distributions are measured in a COULTER 2.00 2.2 in chloroform (powder highly soluble in water). The values given in the table are the mean sizes corresponding to main peaks (bimodal distributions).
The static angle of repose is measured on a cone of powder formed using a calibrated funnel (92.9 mm larger diameter; 15.0 mm smaller diameter; 107 mm high); the funnel is in non-magnetic metal of surface roughness 0.16 µm.

Table A1. Quantity of powder in a lifter as a function of its angular position.
(All the angles are given in **radians**.)

angular position	volume fraction of powder in the lifter
$\gamma_I \le \gamma < \gamma_A$	$\xi = \frac{\beta}{2\pi} - \left(1 - \frac{h_o}{R} - \frac{h_p}{R \cdot \tan(\delta - \gamma)}\right) \cdot \frac{\sin\beta}{2\pi} - \frac{{h_p}^2}{2\pi \cdot R^2 \cdot \tan(\delta - \gamma)}$
$\gamma = \gamma_A = \delta - \tan^{-1}\left(\frac{h_p}{R - h_o}\right)$	$\xi = \frac{\beta}{2\pi} - \frac{(R - h_o) \cdot h_p}{2\pi \cdot R^2}$
$\gamma_A < \gamma < \delta$	$\xi = \frac{\beta}{2\pi} - \left(1 - \frac{h_o}{R}\right)^2 \cdot \frac{\tan\beta}{2\pi} + \left(1 + \left(1 - \frac{h_o}{R}\right) \cdot \frac{1}{\cos\beta}\right) \cdot \left(\frac{h_p}{R} + \left(1 - \frac{h_o}{R}\right) \cdot \tan\beta\right) \cdot \frac{\cos\beta}{2\pi}$
$\gamma = \delta$	$\xi = \frac{\beta}{2\pi} - \left(1 - \frac{h_o}{R}\right)^2 \cdot \frac{\tan\beta}{2\pi} + \left(\frac{h_p}{R} - \left(1 - \frac{h_o}{R}\right) \cdot \tan\beta\right)^2 \cdot \frac{1}{2\pi \cdot \tan\beta}$
$\delta < \gamma < \gamma_B$	$\xi = \frac{\beta}{2\pi} - \left(1 - \frac{h_o}{R}\right)^2 \cdot \frac{\tan\beta}{2\pi} + \left(1 - \left(1 - \frac{h_o}{R}\right) \cdot \frac{1}{\cos\beta}\right) \cdot \left(\frac{h_p}{R} - \left(1 - \frac{h_o}{R}\right) \cdot \tan\beta\right) \cdot \frac{\cos\beta}{2\pi}$
$\gamma = \gamma_B = \delta + \tan^{-1}\left(\frac{h_p}{h_o}\right)$	$\xi = \frac{h_p \cdot h_o}{2\pi \cdot R^2}$
$\gamma_B < \gamma \le \gamma_F$	$\xi = \frac{{h_p}^2}{2\pi \cdot R^2 \cdot \tan(\delta - \gamma)}$
$\gamma = \gamma_F = \delta + \frac{\pi}{2}$	$\xi = 0$

Whatever γ, $\beta = \cos^{-1}\left(\frac{l \cdot \sin^2(\delta - \gamma) + \cos(\delta - \gamma) \cdot \sqrt{R^2 - l^2 \cdot \sin^2(\delta - \gamma)}}{R}\right)$ and $l = R - h_o - \frac{h_p}{\tan(\delta - \gamma)}$

Except for $\gamma = \gamma_A$: $\beta = \tan^{-1}\left(\frac{h_p}{R - h_o}\right)$, for $\gamma = \delta$: $\beta = \sin^{-1}\left(\frac{h_p}{R}\right)$, and for $\gamma \ge \gamma_B$: $\beta = 0$.